

Research article

Strzelecki S.<sup>1,\*</sup><sup>1</sup> ORCID : 0000-0001-5030-5249;<sup>1</sup> Technical University Łódź, Łódź, Poland

\* Corresponding author (stanislaw.strzelecki[at]p.lodz.pl)

**Abstract**

Application of the thrust bearings in different engineering designs generates the problems of thermal state, which generates the wear of the fixed or tilting pads of bearing. These problems can be avoided by application in the design process the proper methods and numerical algorithms that allow the calculation of bearing static characteristics, including the maximum oil film temperature. The knowledge of thermal state of bearing should assure the reliable and durable bearing operation and is important for the designers of thrust bearings.

This paper presents the results of calculations of some static characteristics of tilting-pad thrust bearing, including its maximum oil film temperature under effect of tilt angle of the pad. Numerical solution by means of finite differences was applied for the solution of geometry, Reynolds, energy and viscosity equations. Adiabatic oil film, laminar flow in the bearing gap was considered. The developed numerical algorithm assures the computation of bearing performances, and it creates the tool leading to the solution of thermal problems. Different values of operating speeds were assumed.

**Keywords:** hydrodynamic lubrication, thrust bearings, pad tilt, maximum oil film temperature.

**ЭФФЕКТ УГЛА НАКЛОНЕНИЯ ПЛИТКИ НА МАКСИМАЛЬНУЮ ТЕМПЕРАТУРУ УПОРНОГО ПОДШИПНИКА**

Научная статья

Стшелецкий С.<sup>1,\*</sup><sup>1</sup> ORCID : 0000-0001-5030-5249;<sup>1</sup> Технический Университет Лодзь, Лодзь, Польша

\* Корреспондирующий автор (stanislaw.strzelecki[at]p.lodz.pl)

**Аннотация**

Применение упорных подшипников в различных инженерных конструкциях порождает проблемы теплового состояния, которое приводит к износу неподвижных или наклонных вкладышей подшипника. Избежать этих проблем можно, применяя в процессе проектирования соответствующие методы и численные алгоритмы, позволяющие рассчитывать статические характеристики подшипника, в том числе максимальную температуру масляной пленки. Знание теплового состояния подшипника должно обеспечивать надежную и долговечную работу подшипника и является важным для разработчиков упорных подшипников.

В данной статье представлены результаты расчетов некоторых статических характеристик упорного подшипника с наклонным вкладышем, в том числе его максимальной температуры масляной пленки под действием угла наклона вкладыша. Для решения уравнений геометрии, Рейнольдса, энергии и вязкости применялось численное решение методом конечных разностей. Рассматривалась адиабатическая масляная пленка, ламинарное течение в зазоре подшипника. Разработанный численный алгоритм обеспечивает расчет характеристик подшипника и создает инструмент для решения тепловых задач. В расчетах предполагались различные значения рабочих скоростей.

**Ключевые слова:** гидродинамическая смазка, упорные подшипники, наклон плитки, максимальная температура масляной пленки.

**Introduction**

Tilting pads thrust bearings are applied in the bearing system of the water turbines, main shafts of marine steam turbines, spindles of heavy machine tools, gears, etc. These bearings can transfer large thrust loads from rotating shafts to supporting structures.

Development of modern rotating machinery is strictly bound with an increase in applied loads, higher rotational speed and generated power. From this technical point of view, the knowledge of pad temperature and particularly its maximum temperature is very important.

The maximum oil film temperature is an important limitation that do not allow for any increase in loads and rotational speeds of thrust bearings. The increase in the temperature of the lubricating oil is caused by the amount of heat released in the oil film during the operation of the bearing. Hence, the researchers' interest in thermal phenomena occurring in thrust bearings [1], [2], [3] and [5], [6].

The sliding surface of the tilting pad can be made from the traditional white metal or special polymers. The strengths properties of such materials, their permissible operating temperatures, create limitations on the maximum oil film temperature. Therefore, taking into account thermal phenomena in the process of designing and calculating a bearing seems necessary. An additional problem that is important from the technical point of view is the transition from mixed friction to fluid friction and vice versa during start-up and stopping phase of the machine. The period of mixed friction can generate very inconvenient condition of bearing operation resulting in increase of temperature in oil film [7], [8], [9], [10] and [11], [12], [13].

The tribosystem of thrust bearing consists of tilting or fixed pads and thrust collar, the parts that are separated by the layer of lubricant. The heat generated in the layer of lubricant determines the thermal behaviour of such tribosystem and has a

decisive effect on its reliable operation. Improper choice of bearing geometrical and operational parameters generates thermal problems of wear and finally the failure of bearing and bearing system.

The boundary parameters limiting the operation of thrust bearings are: minimum thickness and maximum temperature of oil film (Fig. 1a); the horizontal line (boundary operation) results from limiting stress levels around the pad pivot [1]. From the point of proper exploitation of rotating machine with tilting pad bearing, the control of the pad temperature is very important. It results from the calculations and measurements of pad temperature that point out on the hot spot region that is placed at the outer edge of the trailing edge. Then, the thermocouple should be located in this region (Fig. 1b and Fig. 1c).

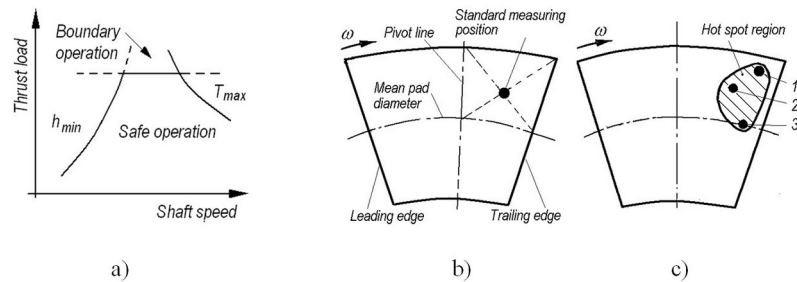


Figure 1 -

Parameters limiting the operation of thrust bearings (a), the regions of largest oil film temperatures (b) and the standard position of temperature measurements (c):

$\omega$  – angular speed of thrust collar; 1, 2, 3 – point of highest temperature; *shadowed field* – range of largest temperatures in oil film

Note: based on [1]

Tilting- or fixed pad temperature information is required by the designers to keep the bearing operation within the temperature limit imposed by the sliding surface of bearing material. Additionally, it allows to evaluate oil film temperature and power loss over a wide range of operating duties.

Thermal problems in different types of journal bearings result from an excessive oil film temperature, thermal gradients generating the bearing distortion, heat flow to and from bearing [5], [6]. An excessive oil film temperature leads to the degradation of lubricant and bearing material [6]. Exemplary damage to the axial part of high-speed axial-radial journal bearing that was caused by an excessive oil film temperature shows Fig. 2 (melted bearing material was transferred into the oil grooves between fixed pads) [4], [5].

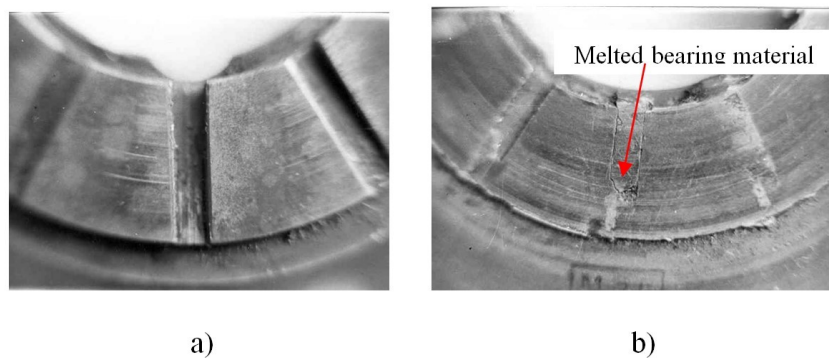


Figure 2 - View of the axial part of radial-axial (fixed pads) bearing of high-speed compressor:  
 a – unloaded side; b – loaded side

Note: melted bearing material in the radial oil grooves

The ground for the safe operation of journal bearings, both radial and axial thrust at proper oil film temperature is the full knowledge of bearing thermal performances particularly the oil film temperature distribution and its maximum value.

Static characteristics of tilting-pad thrust bearing are affected by the geometry of oil film, including the tilt angles of the pad. These angles should be considered in two planes, however one of them, in the direction of pad rotation, is more important and has larger effect on the bearing characteristics.

This paper presents the results of computation of the oil film maximum temperature of thrust bearing under effect of the pad tilt angles. The numerical algorithm for calculation of thrust bearing with tilting pads and the assumptions of laminar and adiabatic model of oil film was applied.

### Oil film thickness, pressure and temperature distributions

The lubricant gap forms an average thickness  $h_s$  which is the result of tilting pad rotation with regard to axes  $x$  and  $y$  intersecting at the point  $s$  with coordinate  $(R_s, \delta_0, h_s)$ ; this point correspond to the support point of pad.

Schematic view of tilting pad geometry shows Fig. 3. Oil film thickness is described by Eq. (1).

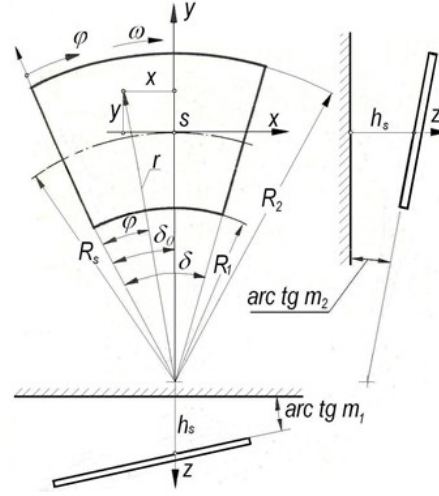


Figure 3 - Schematic view of tilting pad and oil film geometry:

$R_1, R_2$  – inner an outer radius of the thrust tilting pad,  $\delta$  – angle of the thrust tilting pad length

$$\bar{h} = 1 - \frac{m_1 R_s}{h_s} \bar{r} \sin(\bar{\delta}_0 - \bar{\varphi}) + \frac{m_2 R_s}{h_s} [\bar{r} \cos \delta (\delta_0 - \bar{\varphi}) - 1] \quad (1)$$

where:  $\bar{h}$  – dimensionless oil film thickness,  $h_s$  – oil film thickness at the point  $s$  with coordinates  $(R_s, \delta_0)$ ,  $m_1, m_2$  – tangents of pad tilt angle,  $r, \varphi$  – cylindrical system coordinates,  $R_s$  – mean radius of the thrust pad,  $\delta_0$  – angle of the insert support line.

The flow of mass and energy in a lubricating film govern three basic laws: conservation of mass, maintaining the quantity of motion and the energy conservation. Applying these laws, the Navier-Stokes and geometry of oil film equations allow obtaining the Reynolds, energy, viscosity equations [2], [3], [4], [5], [6]; their solution gives the static characteristics of thrust tilting pad bearing for adiabatic or diathermal model of oil film.

Equation (2) describes the distribution of the pressure in the oil film in dimensionless form.

$$\frac{\partial^2 \bar{p}}{\partial \bar{r}^2} + \left( \frac{3}{\bar{h}} \frac{\partial \bar{h}}{\partial \bar{r}} + \frac{1}{\bar{r}} - \frac{1}{\bar{\eta}} \frac{\partial \bar{\eta}}{\partial \bar{r}} \right) \frac{\partial \bar{p}}{\partial \bar{r}} + \frac{1}{\bar{r}^2 \delta^2} \frac{\partial^2 \bar{p}}{\partial \bar{\varphi}^2} = 6 \frac{\bar{\eta}}{\delta \bar{h}^3} \frac{\partial \bar{h}}{\partial \bar{\varphi}} - \left( \frac{3}{\bar{h}} \frac{\partial \bar{h}}{\partial \bar{\varphi}} - \frac{1}{\bar{\eta}} \frac{\partial \bar{\eta}}{\partial \bar{\varphi}} \right) \frac{1}{\delta^2 \bar{r}^2} \quad (2)$$

where:  $\bar{p}$  – dimensionless oil film pressure,  $\bar{r}, \bar{\varphi}$  – coordinates of cylindrical system,  $\delta$  – insert angle,  $\bar{\eta}$  – dimensionless dynamic viscosity of lubricant.

Energy equation transformed into dimensionless form (Eq. 3) gives the oil film temperature distribution.

$$P_e K \left( \bar{q}_r \frac{\partial \bar{T}}{\partial \bar{r}} + q_\varphi \frac{1}{\delta \bar{r}} \frac{\partial \bar{T}}{\partial \bar{\varphi}} \right) = -\bar{k}_1 (\bar{T} - T_c) + \Lambda K \frac{\bar{h}^3}{12 \bar{\eta}} \cdot \left[ \left( \frac{\partial \bar{p}}{\partial \bar{r}} \right)^2 + \frac{1}{\delta^2} \left( \frac{\partial \bar{p}}{\partial \bar{\varphi}} \right)^2 \right] + \Lambda K \frac{\bar{r}^2 \bar{\eta}}{\bar{h}} \quad (3)$$

where:  $\bar{T}$  – temperature,  $P_e$  – Peclet number  $P_e = \rho c_v h_s^2 \omega / \lambda$ ,  $c_v$  – specific heat of oil,  $\rho$  – oil density,  $K$  – heat transfer coefficient,  $K = \lambda h s k_{10} / T_c$ ,  $T_c$  – average temperature of oil film,  $\lambda$  – thermal conductivity coefficient of the oil,  $\bar{q}_r, \bar{q}_\varphi$  – flow of oil in radial and peripheral directions.

The dimensionless viscosity of lubricant describes exponential Eq. (4) [4].

$$\bar{\eta} = e^{A(\bar{T} - \bar{T}_0) + B(\bar{T} - \bar{T}_0)^2} \quad (4)$$

where:  $A, B$  – factors including the influence of temperature on the oil viscosity,  $T_0$  – reference temperature.

Iterative solution of equations (1) through (4) gives the fields of oil film pressure, temperature and viscosity. Application of the parabolic approximation [4], [5], [6] allows determination of temperature values  $T(\varphi, z)$  on the boundaries of bearing. In the regions of negative pressure of oil film and on the bearing edges, nil pressure values were considered, i.e.  $p(\varphi, \bar{z}) = 0$ .

The system of equations (1) through (4) was solved numerically by means of finite difference method. It was found that the sufficient accuracy of computation can be obtained applying the net with the number of nodes  $l \times m = 11 \times 21$ . In order to find the discrete values of the functions at individual mesh nodes, the equations (2) and (3) were transformed into the form of differential equations. In the pressure distribution equation (2), the derivatives were replaced by the (central) difference quotients: In case of the energy equation (3), it was more convenient to use backward difference quotients [4], [14], [15].

## Results and discussion of calculations

Developed numerical algorithm allows calculation of the bearing static characteristics, i.e. oil film thickness, pressure, temperature and velocity distribution as well as the quantities characterizing such properties as: bearing load capacity, friction torque, coordinates of oil film resultant force, oil streams as well as maximum values of pressure and temperature.

The following geometrical data were assumed: oil film thickness  $h_s$  at the point with coordinates  $(R_s, \delta_0)$ , inner and outer radius of the plate  $R_1$  and  $R_2$ , tangents  $m_1$  and  $m_2$  of tilt angle of pad with regard of axis  $s_y$  and  $s_x$ ,  $\delta$ ,  $\delta_0$  – angle of pad and angle of supported line, were assumed respectively. Operational data were as follows: dynamic oil viscosity coefficient  $\eta$ , dynamic oil viscosity coefficient at the reference temperature  $\eta_0$ , thermal conductivity coefficient in the oil  $\lambda$ , thermal conductivity coefficient in the pad  $\lambda_t$ , factors  $a$ ,  $b$  including an effect of temperature on the oil viscosity, average temperature of oil film  $T_c$ , reference temperature  $T_0$ , temperature of oil at inlet edge  $T_p$ , heat transfer coefficient  $k$ . The range of rotational speeds varied from 50 rpm through 1000 rpm.

Different pad tilt coefficients  $m_1$  and  $m_2$  were considered. Dimensions of tilt pad: inner, external and mean radius were  $r_1=0,10915$  and  $r_2=0,20915$ ,  $r_{\text{mean}}=0,1592$  respectively.  $T_0=20^\circ\text{C}$ ,  $\eta_0=0,297 \text{ Nsm}^{-2}\rho_0=898\text{kg/m}^3$ ,  $c_p=1980\text{J/kg}^\circ\text{C}$ ,  $\lambda=0,1450 \text{ J/ms}^\circ\text{C}$ . Assumed nodes number were: peripheral direction  $m=21$  and radial direction  $n=6$ .

Exemplary results of computations that were obtained at assumed bearing parameters are given in Fig. 4 through Fig. 15; in these figures, the oil film thickness at the point with the coordinates  $(R_s, \delta_0)$   $h_s$  was assumed as  $0,213\text{E}-03$ . Dimensionless oil film thickness at assumed values of tilt angles  $m_1=-0,0013685$  and  $m_2=0,00076$  shows Fig. 4; the lowest values are at the trailing edge of pad ( $j=21$ ).

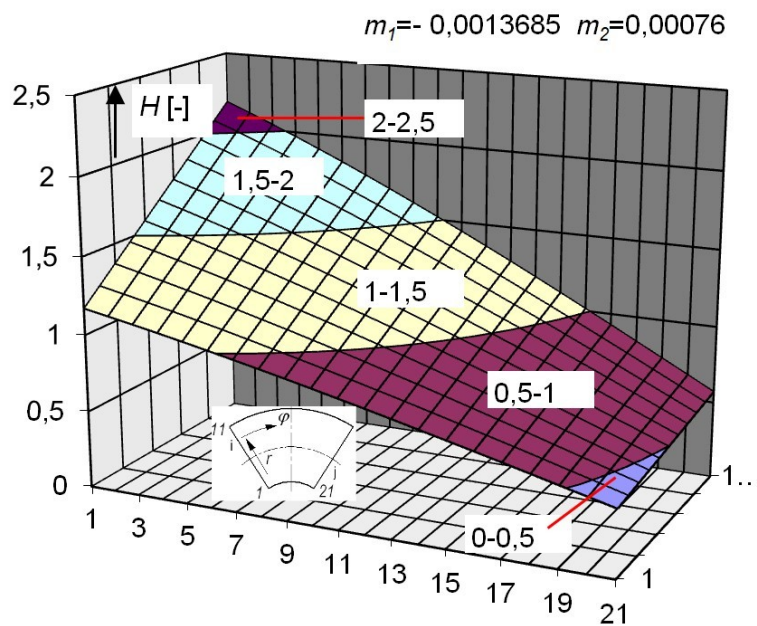


Figure 4 - Dimensionless oil film thickness at assumed values of tilt angles of tilting pad

Figure 5 through Fig. 7 show the oil film pressure distributions on the thrust tilting pad. Three-dimensional pressure field on the pad illustrates Fig. 5. The isobars of pressure (at rotational speed  $n=100 \text{ rpm}$ ) present Fig. 6; maximum value (mesh points  $i=11$  and  $j=21$ ) is observed in the region of external part of pad trailing edge and in the direction of thrust collar rotation. Oil film pressure distribution in peripheral direction and for different radial coordinates shows Fig. 7; pad tilt in two directions was assumed and maximum value of oil film pressure is  $p_{\text{max}}=0,16 \text{ MPa}$  at the coordinates  $i=9$  and  $j=19$ .

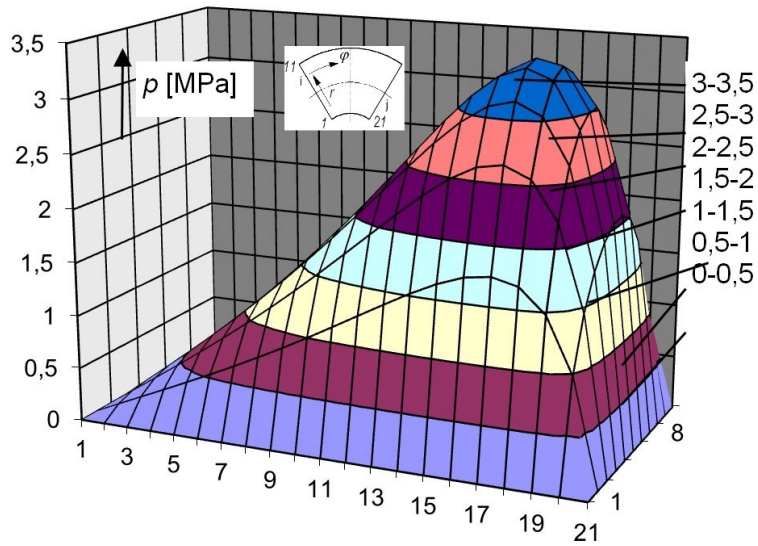


Figure 5 - 3D oil film pressure distribution on the thrust-tilting pad

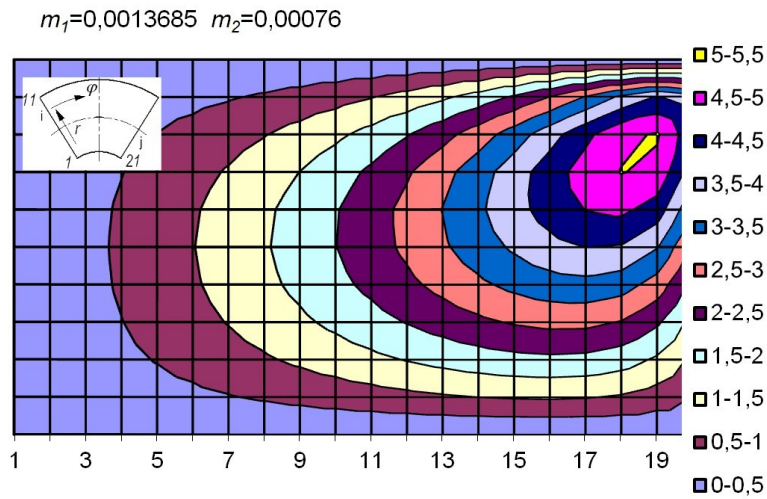


Figure 6 - Isobars of oil film pressure on the tilting pad

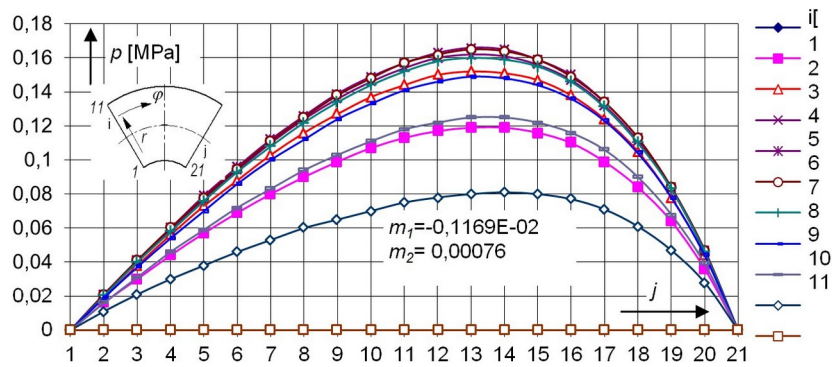


Figure 7 - Oil film pressure distribution in the peripheral direction on the tilting pad

Oil film temperature distribution on the tilting pad and its isotherms present Fig. 8 and Fig. 9 respectively; for assumed bearing parameters; the temperatures of oil film are in the range of 40°C to 51°C and maximum temperature is placed at the coordinates  $i=11$  and  $j=21$  (trailing edge of pad).



An effect of tilt angle  $m_2$  on maximum value of oil film pressure  $p_{max}$  and temperature  $T_{max}$  at different rotational speeds of thrust collar and for constant value of  $m_1$  show Fig.10a ( $m_1 \neq 0, m_2 = 0$ ) and Fig. 10b ( $m_1 \neq 0$  and  $m_2 = 0$ ). In both cases, an increase in the rotational speeds causes the increase in  $p_{max}$  and  $T_{max}$ . However, nil value of tilt angle  $m_2$  generates higher  $T_{max}$  (e.g. at  $n=300$  rpm and for  $m_1=-0,01469$  and  $m_2=0$  then  $T_{max} \approx 55^\circ\text{C}$ , but  $T_{max} \approx 45^\circ\text{C}$  at  $m_1=-0,01469$  and  $m_2=-0,0007$ ).

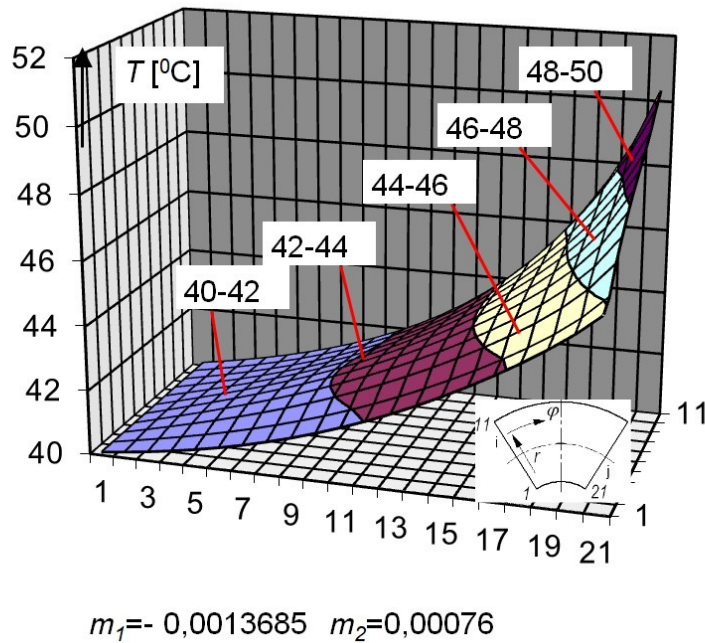


Figure 8 - Oil film temperature distribution (3D) on the tilting pad

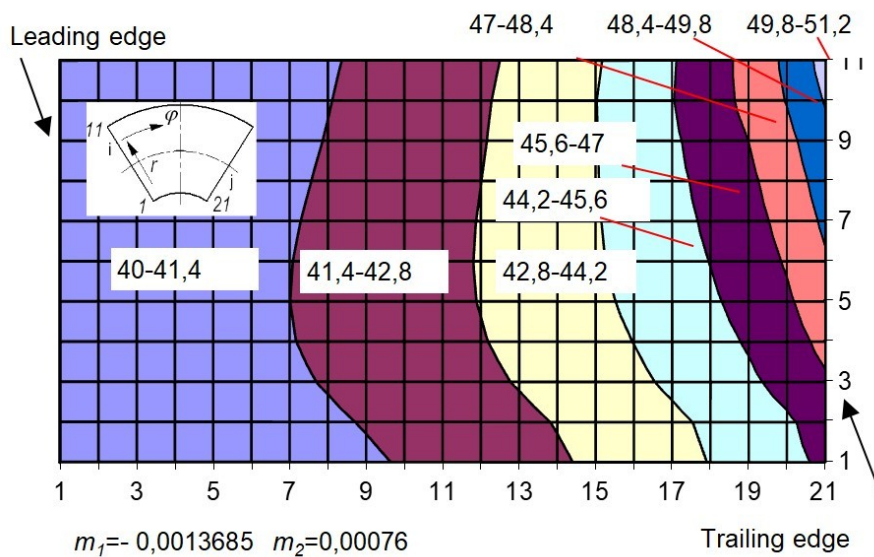


Figure 9 - Isotherms (in  $^\circ\text{C}$ ) of oil film temperature distribution on the tilting pad

Note: – upper part of temperature field close to the trailing edge

Figure 11 shows maximum oil film temperature versus pad tilt angle  $m_1$  at different rotational speeds of thrust collar and assumed values of pad tilt angles  $m_2$ . In case of  $m_2$  equal nil, the pad tilt angle is in the range up to 0,002 (Fig. 11a). However, when  $m_2$  is larger than nil the tilt angle  $m_1$  of the pad is in wider range, up to 0,0025 (see Fig. 11a and Fig. 11b). However, at  $m_2=0,0$  the pad tilt angle  $m_1$  should be used up to the approximate value 0,0018 because the maximum temperature reaches the value almost  $90^\circ\text{C}$  (Fig. 11a). In case of  $m_2 > 0$  the maximum temperature  $90^\circ\text{C}$  occurs at the pad tilt angle approximately 0,0023 (Fig. 11b – see rotational speed 500rpm).

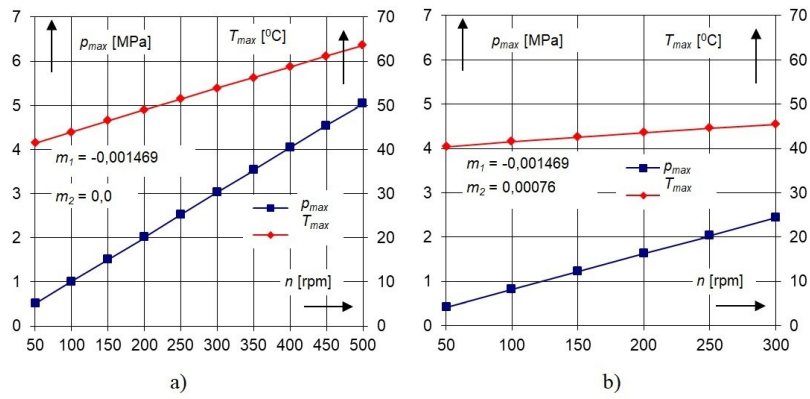


Figure 10 - Maximum oil film pressure and temperature versus different rotational speeds of thrust collar for pad tilt angles:  
 a –  $m_1 \neq 0, m_2 = 0$ ; b –  $m_1 \neq 0$  and  $m_2 \neq 0$

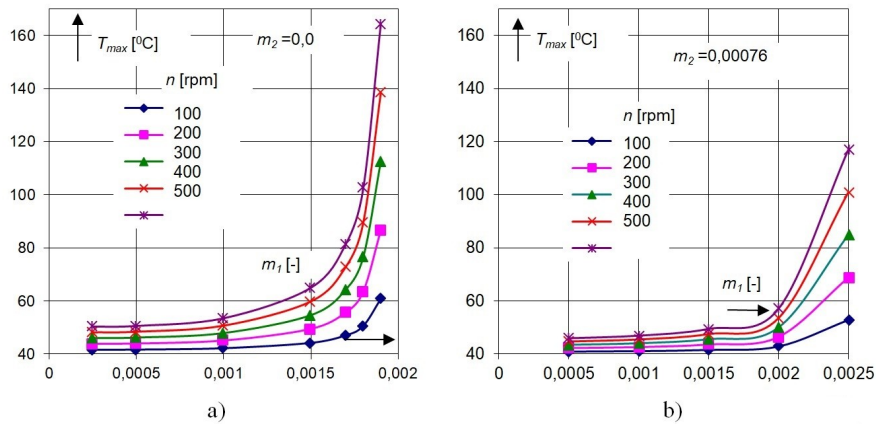


Figure 11 - Maximum oil film temperature versus pad tilt angles  $m_1$  and for different tilt pad angles  $m_2$ :  
 a –  $m_2 = 0,0$ ; b –  $m_2 = 0,00076$

Maximum oil film temperature versus oil film thickness  $h_s$  at pad support point and different rotational speed of thrust collar tilt and assumed values of pad tilt angles  $m_1$  and  $m_2$  shows Fig. 12. In both cases, maximum oil film temperature shows the decrease at the increase in  $h_s$ . At the assumed value of  $m_1$  and for  $m_2 = 0$  (Fig. 12a) or  $m_2 \neq 0$  (Fig. 12b) there is an increase in maximum temperatures of oil film with increasing rotational speeds. However, this increases if characterized by higher temperatures in case of  $m_2 = 0$  (Fig. 12a) and lower temperatures when  $m_2 \neq 0$  (Fig. 12b).

Effect of different rotational speeds of thrust collar on the maximum oil film temperature for assumed pad tilt angles illustrates Fig. 13 (a – constant  $m_1$ , b – constant  $m_2$ ).

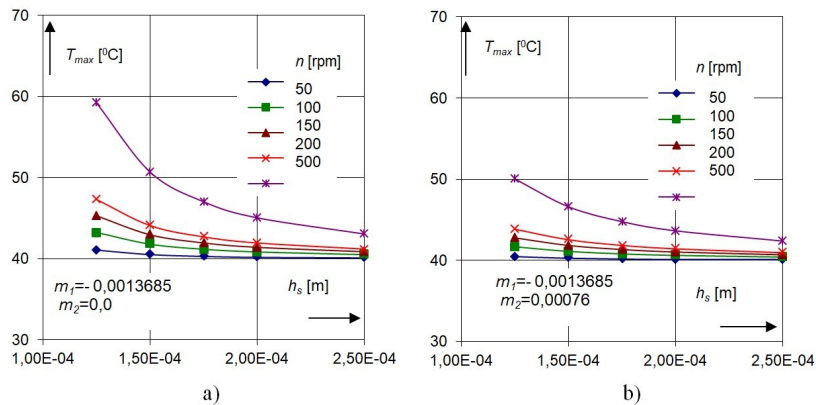


Figure 12 - Maximum oil film temperature versus assumed oil film thickness  $h_s$  for different rotational speeds of thrust collar at assumed value of  $m_1$  and different values of  $m_2$ :  
 a –  $m_2 = 0,0$ ; b –  $m_2 = 0,00076$

Note: oil film temperature at the pad inlet was  $T_p=40^{\circ}\text{C}$

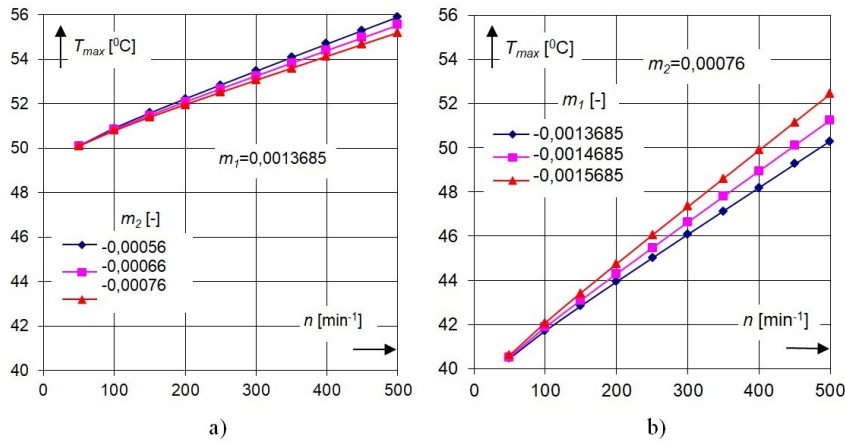


Figure 13 - Effect of rotational speed of thrust collar on the maximum oil film temperature for different pad tilt angles  $m_1$ :  
 a – constant  $m_1$ ; b – constant  $m_2$

On the assumption of different, both tilt angles  $m_1$  and  $m_2$ , the maximum oil film temperature shows almost linear run (Fig. 14); these temperatures are increasing with the increase in rotational speed of thrust collar.

However, when the tilt angle of pad  $m_1$  is larger than nil and the angle  $m_2=0,0$  then the different run of temperatures is observed (Fig. 15); there is almost no difference in the maximum temperatures of runs for close values of  $m_1$  (Fig. 14 the lines 1 and 4). In this discussed case, the maximum temperatures of oil film are lower as compare to the case in which the angles  $m_1$  and  $m_2$  differ from nil.

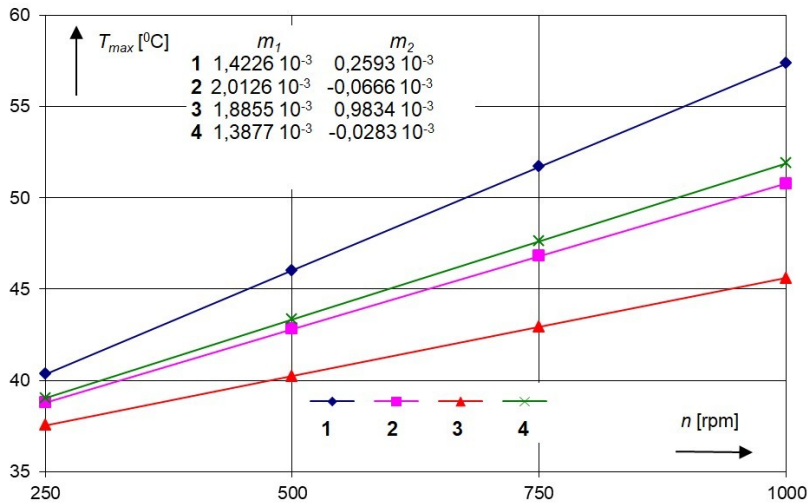


Figure 14 - Effect of different pad tilt angles on the maximum oil film temperature of pad versus rotational speeds of thrust collar

Note: based on [3]



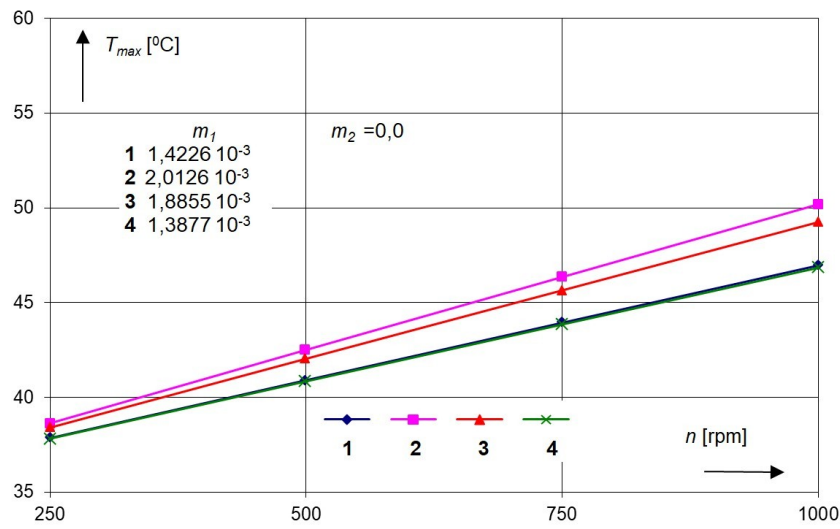


Figure 15 - Effect of different pad tilt angles  $m_1 \neq 0$  at  $m_2 = 0,0$  on the maximum oil film temperature of pad versus rotational speeds of thrust collar

It results from Fig. 14 and Fig. 15 that there is a larger increase in the maximum oil film temperatures when both tilt angles are greater than nil. Considering, e.g. two cases, the first with the angle  $m_1=1,4226E-3$  and  $m_2=0,2593E-3$  (Fig. 14) and the second case when  $m_1=1,4226E-3$  and  $m_2=0,0$  (Fig. 15) it can be stated that the increase in maximum temperature is larger in the first case; it certifies the necessity to consider both angles of pad tilt in calculations of thrust tilting pad bearings.

Figure 16 shows maximum oil film temperature versus rotational speeds of thrust collar at assumed value of oil film thickness and tilting pad angles.

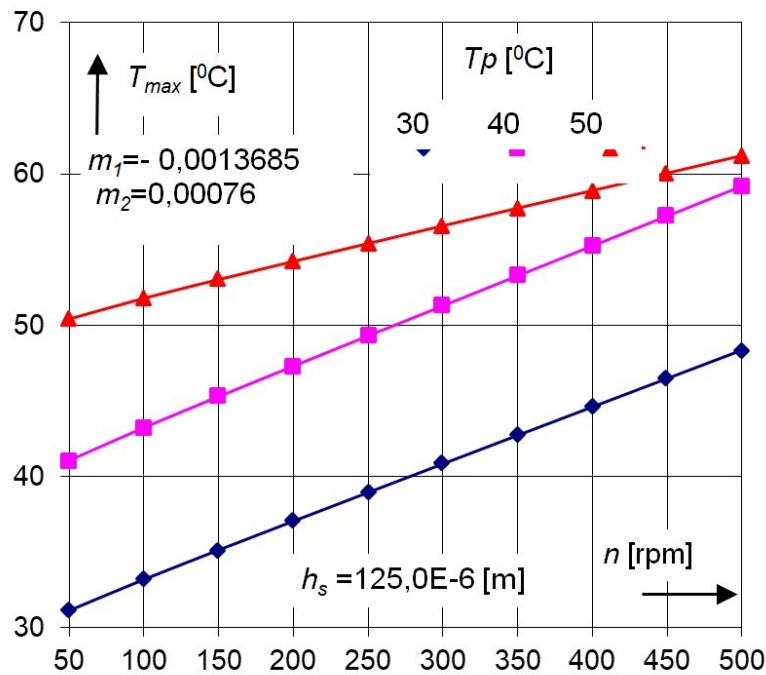


Figure 16 - Maximum oil film temperature versus rotational speed of thrust plate at assumed value of oil film thickness

It results from Fig. 16 that at lower temperatures of supplied lubricant there is similar increase in temperatures for considered rotational speeds of thrust collar (Fig. 16, increases for the temperatures  $30^\circ\text{C}$  and  $40^\circ\text{C}$ ; are  $17,22^\circ\text{C}$  and  $18,14^\circ\text{C}$ , respectively). However, at the temperature of supplied lubricant equal to  $50^\circ\text{C}$  an increase in maximum oil film temperature is  $10,8^\circ\text{C}$  (Fig. 16, upper line for  $50^\circ\text{C}$ ).

### Conclusion

Theoretical calculations and experimental data, as well as the analysis of the results obtained from these studies, allow the formulation of the following conclusions:

1. The geometry of the oil film expressed by the tilt angles of the pad has a significant effect on the operating characteristics of the axial thrust bearing.

2. Pad tilt parameters  $m_1$  and  $m_2$  at an assumed film thickness at the point of pad support cause the changes in oil film temperature distribution and its maximum values.

3. An increase in the rotational speed of the thrust collar causes the increase in maximum oil film temperature at the increase of pad tilt angles.

4. The isobars and the isotherms of oil film pressure and temperature distribution on the tilting pad point on their maximum value positions, which are placed at trailing edge, upper region of tilting pad.

5. Higher temperatures of supplied lubricant assure smaller increase in its maximum temperatures at the increase in rotational speeds of the thrust plate.

6. A thermocouple controlling the maximum oil film temperature should be placed in the hot spot region of the pad. Such solution is very important for reliable operation of thrust bearing.

In the process of bearing design, it is necessary to take into account two angles of tilt pad and analyse the obtained maximum temperatures of oil film. The results giving higher temperatures of oil film and maximum temperatures should be considered as more extreme case. In such situation, the design of bearing should be more resistant against accidental overriding of permissible temperatures of operation.

### **Конфликт интересов**

Не указан.

#### **Рецензия**

Все статьи проходят рецензирование. Но рецензент или автор статьи предпочли не публиковать рецензию к этой статье в открытом доступе. Рецензия может быть предоставлена компетентным органам по запросу.

### **Conflict of Interest**

None declared.

#### **Review**

All articles are peer-reviewed. But the reviewer or the author of the article chose not to publish a review of this article in the public domain. The review can be provided to the competent authorities upon request.

### **Список литературы / References**

1. Horner D. Measurements of Maximum Temperature in Tilting-Pad Thrust Bearings / D. Horner, J. E. I. Simons, S. D. Advani. — STLE Transactions. — 1997. — Vol. 31. — P. 44–55.
2. Kusmierz L. Analiza odkształceń sprężystych klocków przechylnych na charakterystyce pracy osiowego łożyska oporowego / L. Kusmierz. — Łódź : Politechnika Łódzka, 1980.
3. Murdzia E. Charakterystyka Termohydrodynamiczna łożyska oporowego / E. Murdzia. — Łódź : Politechnika Łódzka, 1980.
4. Strzelecki S. łożyska Poprzeczne. Identyfikacja charakterystyki pracy łożysk promieniowych Wielopłatowych, hydrodynamicznych / S. Strzelecki. — Wydawnictwo Politechniki Śląskiej : Gliwice, 2021.
5. Ghoneam S. M. Thermal Problems of Multilobe Journal Bearings / S. M. Ghoneam, S. Strzelecki // Meccanica. — 2006. — № 41. — P. 571–579.
6. Wasilczuk M. łożyska osiowe o dużych gabarytach / M. Wasilczuk // Radom. — Dom Wydawniczy Instytutu Technologii i eksploatacji, 2012.
7. Glavatski S. B. TEHD Analysis of Tilting-Pad Thrust Bearings – Comparison with Experimental Data / S. B. Glavatski, M. Fillon // Synopses of the International Tribology Conference Nagasaki. — 2000.
8. Fillon M. Effect of presence of lifting pocket on the THD performance of a large tilting-pad thrust bearing / M. Fillon, M. Wodtke, M. Wasilczuk // Journal of Friction and Wear. — 2015. — Vol. 3(4). — P. 266–274.
9. Wodtke M. Large hydrodynamic thrust bearing: Comparison of the calculations and measurements / M. Wodtke, A. Schubert, M. Fillon [et al.] // J-journal of engineering tribology. — 2014. — № 228. — P. 974–983.
10. Bouyer J. Experimental research on a hydrodynamic thrust bearing with hydrostatic lift pockets: Influence of lubrication modes on bearing performance / J. Bouyer, M. Wodtke, M. Fillon // Tribology international. — 2022. — Vol. 165. — Art. 107253.
11. Wodtke M. Study of the Influence of Heat Convection Coefficient on Predicted Performance of a Large Tilting-Pad Thrust Bearing / M. Wodtke, M. Fillon, A. Schubert [et al.] // Journal of tribology-transactions of the asme. — 2013. — Vol. 135. — P. 1–11.
12. Chmielowiec-Jabłczyk M. Improvement of the thrust bearing calculation considering the convective heating within the space between the pads / M. Chmielowiec-Jabłczyk, A. Schubert, C. Kraft [et al.] // 16th EDF/Prime Workshop: Behaviour of journal and thrust bearings under transient and mixed lubrication regime. — 2017. — P. 1–12.
13. Rotta G. Modelling lubricant flow between thrust-bearing pads / G. Rotta, M. Wasilczuk // Tribology international. — 2008. — Vol. 41. — P. 908–913.
14. Murdzia E. Computer program of the computation of tilting-pad thrust bearings / E. Murdzia, S. Strzelecki. — 2020.
15. Murdzia E. Calculation of Tilting-Pad Thrust Bearings / E. Murdzia, S. Strzelecki // Tribology international. — 2021. — № 298. — P. 27–36.

### **Список литературы на английском языке / References in English**

1. Horner D. Measurements of Maximum Temperature in Tilting-Pad Thrust Bearings / D. Horner, J. E. I. Simons, S. D. Advani. — STLE Transactions. — 1997. — Vol. 31. — P. 44–55.
2. Kusmierz L. Analiza odkształceń sprężystych klocków przechylnych na charakterystyce pracy osiowego łożyska oporowego [Analysis of elastic deformations of tilting pads on the operating characteristics of axial thrust bearing] / L. Kusmierz. — Łódź : Lodz University of Technology, 1980. [in Polish]
3. Murdzia E. Charakterystyka Termohydrodynamiczna łożyska oporowego [Thermohydrodynamic characteristics of thrust bearing] / E. Murdzia. — Lodz : Lodz University of Technology, 1980. [in Polish]

4. Strzelecki S. Łożyska Poprzeczne. Identyfikacja charakterystyki pracy łożysk promieniowych Wielopłatowych, hydrodynamicznych [Journal Bearings. Identification of the Operating Characteristics of Multilobe, Hydrodynamic Radial Bearings] / S. Strzelecki. — Publishing House of the Silesian University of Technology : Gliwice, 2021. [in Polish]
5. Ghoneam S. M. Thermal Problems of Multilobe Journal Bearings / S. M. Ghoneam, S. Strzelecki // *Meccanica*. — 2006. — № 41. — P. 571–579.
6. Wasilczuk M. łożyska osiowe o dużych gabarytach [Large overall dimensions axial thrust bearings] / M. Wasilczuk // Radom. — Scientific Publisher House of the Institute of Technology and Exploitation, 2012. [in Polish]
7. Glavatski S. B. TEHD Analysis of Tilting-Pad Thrust Bearings – Comparison with Experimental Data / S. B. Glavatski, M. Fillon // *Synopses of the International Tribology Conference Nagasaki*. — 2000.
8. Fillon M. Effect of presence of lifting pocket on the THD performance of a large tilting-pad thrust bearing / M. Fillon, M. Wodtke, M. Wasilczuk // *Journal of Friction and Wear*. — 2015. — Vol. 3(4). — P. 266–274.
9. Wodtke M. Large hydrodynamic thrust bearing: Comparison of the calculations and measurements / M. Wodtke, A. Schubert, M. Fillon [et al.] // *J-journal of engineering tribology*. — 2014. — № 228. — P. 974–983.
10. Bouyer J. Experimental research on a hydrodynamic thrust bearing with hydrostatic lift pockets: Influence of lubrication modes on bearing performance / J. Bouyer, M. Wodtke, M. Fillon // *Tribology international*. — 2022. — Vol. 165. — Art. 107253.
11. Wodtke M. Study of the Influence of Heat Convection Coefficient on Predicted Performance of a Large Tilting-Pad Thrust Bearing / M. Wodtke, M. Fillon, A. Schubert [et al.] // *Journal of tribology-transactions of the asme*. — 2013. — Vol. 135. — P. 1–11.
12. Chmielowiec-Jabłczyk M. Improvement of the thrust bearing calculation considering the convectional heating within the space between the pads / M. Chmielowiec-Jabłczyk, A. Schubert, C. Kraft [et al.] // *16th EDF/Prime Workshop: Behaviour of journal and thrust bearings under transient and mixed lubrication regime*. — 2017. — P. 1–12.
13. Rotta G. Modelling lubricant flow between thrust-bearing pads / G. Rotta, M. Wasilczuk // *Tribology international*. — 2008. — Vol. 41. — P. 908–913.
14. Murdzia E. Computer program of the computation of tilting-pad thrust bearings / E. Murdzia, S. Strzelecki. — 2020.
15. Murdzia E. Calculation of Tilting-Pad Thrust Bearings / E. Murdzia, S. Strzelecki // *Tribology international*. — 2021. — № 298. — P. 27–36.